Author Accepted Manuscript version of the paper by Siamak Karimi, Mehdi Zadeh and Jon Are Suul.
in IEEE transactions on industry applications, 59 (2023) Page 4752-4763,
http://dx.doi.org/10.1109/TIA.2023.3258419

Operation-based Reliability Assessment of Shore-to-Ship Charging Systems Including On-Shore Batteries

Siamak Karimi, Mehdi Zadeh, and Jon Are Suul

***Abstract*—In this paper, an operation-based reliability assessment framework is proposed for Shore-to-Ship Charging (S2SC) systems including On-Shore Batteries (OSB). The OSB is considered to support the grid under fast charging loads. By the proposed approach, the impact of operational planning on reliability is identified. The main operational parameters considered in the reliability analysis include the charging load power and the charging- and discharging scheduling of the OSB. A hierarchical reliability framework is established where the failure rates of the components are estimated based on the FIDES methodology for physics-of-failure-based reliability prediction. Then, a dynamic failure threshold is introduced to translate the component failure consequences to the system performance into three states – failed, normal, and de-rated operation. Hence, the failure threshold is obtained for a specific set of operational and system design parameters. Additionally, to benchmark the characteristics of the SoC profiles of the OSB, an operation-based battery lifetime analysis is conducted. The evaluation of system-level reliability and on-shore battery lifetime is carried out for a 4MW dc S2SC system with a specified range of operation parameters. The results show that batteries and the IGBTs in the power electronics converters are the most reliability-critical elements. Moreover, it is apparent from the results that adjustments to the OSB power profile planning can potentially improve the reliability of the system for specific system sizing. It is also found that the OSB lifetime can be extended up to 2.5 times by increasing the capacity by 50 % and keeping the SoC close to around 50%.**

***Index Terms*—marine electrification, shipboard power systems, battery-electric ship, shore-to-ship charging, reliability assessment.**

I. Introduction

Shore-to-Ship Charging (S2SC) contributes to reducing the emissions from sea transportation by enabling the use of onboard batteries for supporting or replacing fossil-fuel-based engines [1], [2]. With the availability of sustainable energies, i.e., hydropower, solar, and wind energy, from the onshore grid, the plug-in battery-electric marine vessels can operate in low- or zero-emission mode, thanks to the S2SC systems [3]. Currently, Approximately 50% of all the marine vessels in operation or in order with onboard batteries need S2SC infrastructure [4]. The dominant vessel types among these ships are the car/passenger ferries. Such short-distance vessels operate on a tight schedule for commuting passengers and cars. Therefore, the On-Board Batteries (OBB) installed in such vessels are recharged between the transits within a critical time window by high-power charging, and during the night by relatively low-power charging [3]. An S2SC system has a Grid Interface (GI) as the main source of the charging power. Moreover, On-Shore Batteries (OSB) can be installed to support the grid for providing fast charging loads [5].

Since a plug-in battery-electric ship is vitally dependent on its S2SC system, failures in the S2SC system can adversely affect the vessel operation. As a result, the ship operator may be charged with costly penalties from the transportation authorities in case of delays or cancellations [6]. Frequent interruptions of the regular schedules can also damage the reputation of route-based passenger/car ferry transportation if passengers are dissatisfied. [7]. Furthermore, the capital cost of S2SC infrastructures is relatively high. Therefore, S2SC failures invoking unplanned maintenance efforts or replacements can reduce long-term revenues.

An S2SC system is dominantly made up of reliability-critical components, including power electronics converters and batteries [5]. Therefore, the reliability of S2SC should be modeled and considered for design and operation in addition to the other influencing factors, including cost and energy efficiency. Integrating reliability estimation in system configuration design routines of S2SC can decrease the chances of system failures in advance if the choice of the system elements and configurations are decided based on their impact on the estimated probability for failures [8]. As measures to achieve higher reliability, calculation of optimal redundancy, over-sizing, and modifications of the system topology have been suggested by various research studies [9], [10]. However, most of these measures include adding extra components and redundant units which increases the already high investment costs. Another approach can be to incorporate considerations on reliability into the operational planning for providing power references and battery scheduling of the S2SC system. By doing so, the system reliability can be enhanced without adding extra components or introducing changes in the system configuration.

To model the reliability of S2SC systems, various methods, including, the reliability block diagram and Markov chain analysis, can be employed by applying the historical-data-based failure rates of the parts and components [11]. The

Manuscript received 12 Jul 2022; revised 16 Oct 2022; revised 18 Jan 2023; accepted 14 Feb 2023. This work was supported by SFI-smart maritime, Norway. (Corresponding author: Mehdi Zadeh.)

S. Karimi and M. Zadeh are with the Department of Marine Technology, Norwegian University of Science and Technology (NTNU), 7050 Trondheim, Norway (e-mails: siamak.karimi@ieee.org; mehdi.zadeh@ntnu.no). J. A. Suul is with SINTEF Energy Research, and also with the Department of Engineering Cybernetics, Norwegian University of Science and Technology (NTNU), Norway (e-mail: jon.a.suul@sintef.no).

reliability of a power system is usually quantified by general metrics such as the mean time to the failure, Loss of Load Expectation (LOLE), or System Average Interruption Duration Index (SAIDI) [12]. As discussed in [7], such reliability indices can be redefined To better capture the specific behaviors of an S2SC system. Suitable indicators can, for instance, be associated with the probability of accomplishing the charging missions such that the vessel can operate with its OBB recharged according to the schedule [13].

Previous studies have extensively investigated the failure modeling of power electronic devices, in particular, semiconductor devices and capacitors, to be used for estimating the reliability of power electronic converters [14]. The latest advancements in semiconductor technologies, converters, as well as converter design, require accurate aging and lifetime prediction [15]. However, due to the complexity and lack of available data regarding such experimental models, reliability handbooks, such as MIL-HDBK-217F, RDF2000, GJB200, 217Plus, and FIDES, are still being widely used, especially for the reliability analysis of systems with multiple power converters [16], [17].

Conventionally, to estimate the constant failure rates of power electronics elements, the data provided in MIL-HDBK-217F is commonly used [7]. Despite the popularity of this approach in various applications, it is not possible to capture the actual operating conditions of the elements, i.e., thermal cycling and the corresponding failure mechanisms [18]. However, the FIDES approach, as one of the most recent reliability handbooks for electrical components, takes into account the physics-of-failure for estimating the failure rates [19]. Additionally, in the FIDES method, the electrical, mechanical, and thermal over-stress factors are considered to predict failure rates in a more accurate way [17], [19]. Battery lifetime is strongly influenced by the thermal environment, the SoC, as well as the power profile of the battery [20]. Nonetheless, the battery failure rate model in the FIDES handbook is not able to fully capture the impact of the SoC profile on battery reliability. To address this, as a complementary approach to the reliability models, the lifetime model of the batteries can be taken into account to benchmark the SoC profiles [16].

Regarding the system-level reliability assessments of power-electronics-based systems under operation, there have been numerous publications that can be inspiring for the study of S2SC systems [18], [21]–[24]. The authors in [21] and [18] assess the reliability of a power-electronics-based system by considering the mission profile. However, the impact of operational planning on reliability was not investigated in those papers. In [22], a reliability-based power-sharing strategy for the converters in a dc microgrid is proposed. Moreover, lifetime-based power control for converters in more-electric aircraft is introduced in [23]. The authors in [24] proposed four energy management strategies for a microgrid that can improve reliability performances. The same procedures as in [22] and [23] can be adapted for an S2SC system since it can be considered a reliability-sensitive multi-converter system with a mission profile.

Regarding reliability studies for S2SC systems, only a few research papers can be found in the literature [7], [13], [25]. In [7], the reliability of dc and ac S2SC systems are assessed by the Markov chain approach, and several application-specific reliability indices are introduced. Moreover, based on the same reliability indices, a design-based reliability framework for S2SC systems is proposed in [13]. That work provided a platform for reliable design and sizing of the S2SC systems supported by OSB. However, the effect of operation planning on the reliability of such systems has not been covered.

According to the aforementioned challenges and the latest available literature, the following research gaps can be identified:

1) The reliability assessments carried out for S2SC systems are mainly aimed at system design and comparison of power system configurations. The impact of charging planning on reliability, especially considering the power and energy profile planning of OSB in an S2SC, has not been thoroughly investigated yet.
2) The reliability data used in the previous works are based on the worst-case operating points. Consequently, they are not suitable for operational profile planning.
3) In the earlier S2SC reliability studies the failure threshold is defined as the minimum power required for keeping the SoC of OBB above the safety limit during the day. Since the change of operational parameters can affect the energy balance constraints in both OBB and OSB, it is hard to use the reliability framework designated for the physical design and system sizing for operation planning. To perform an operation-based reliability assessment, this threshold must be redefined.

A preliminary operation-based reliability evaluation for S2SC systems was presented in [25] in which two scenarios for the discharging and recharging planning of the OSB were tested in terms of reliability and based on the dynamic failure threshold. Further, the impact of the overnight charging of OSB on reliability was studied. In this paper, the work from [25] is extended to give a generalized operation guideline to secure the reliability of the system under various operating scenarios and mission profiles.The main contributions are listed in the following.

1) An operation-based reliability assessment of S2SC systems based on the FIDES reliability models is developed. The reliability is obtained as a function of selected operational parameters, particularly the OSB power profile. This includes the load sharing between the grid and the OSB, the OSB recharging power between the vessel trips, and the OSB overnight charging power. By this approach, more of the design space is swept compared to the limited scenarios considered in [25].
2) To construct the operation-based reliability assessment, a dynamic failure threshold approach is developed. This approach translates the component failure occurrences to the vessel's operation consequences, considering the OBB and OSB energy balances and their SoC safety constraints.
3) The impact of the OSB energy profile planning, including the Depth of Discharge (DoD) and the SoC cycle range, on its battery lifetime is investigated. Accord-

Author Accepted Manuscript version of the paper by Siamak Karimi, Mehdi Zadeh and Jon Are Suul.
in IEEE transactions on industry applications, 59 (2023) Page 4752-4763,
http://dx.doi.org/10.1109/TIA.2023.3258419

ingly, relevant suggestions to improve the lifetime by adjusting the SoC profile of the OSB are given. Here, an experimentally verified calendar and cycling aging model for the Nickel Manganese Cobalt (NMC) Li-ion battery cell is employed to investigate the effect of the SoC profile of the marine batteries on their lifetime [26].

The developed models are applied for evaluating the system reliability under operation while considering the power management parameters, assuming that the physical design and sizing are already decided.

II. Shore-to-ship Charging Systems

This section describes the system configuration and operational analysis of the shore-to-ship charging system under study.

A. System Configuration

An OSB-supported dc S2SC system for a battery-electric ferry is chosen as the case study in this work. This system is inspired by the real-case S2SC system developed for E-ferry Ellen in Denmark [27]. The studied S2SC can supply 4MW and a simplified single-line diagram of the case study is depicted in Fig. 1. In the reliability analysis, a particular focus is given to onshore sub-systems such as GIs and OSBs.

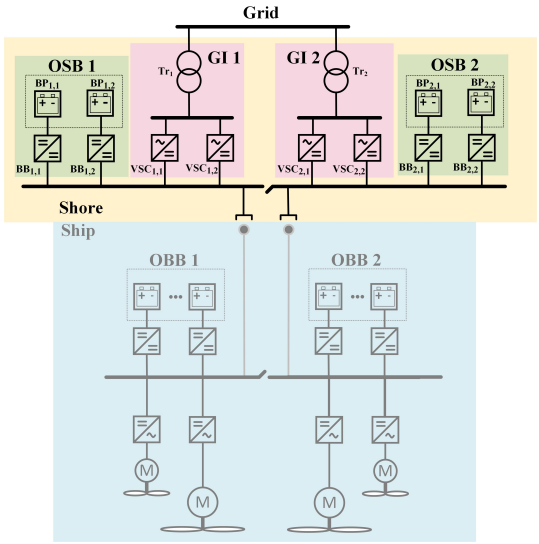

Fig. 1. The S2SC system under study.

The schematic of the Voltage Source Converters ($VSC_{i,j}$) in the GI sub-system, the bidirectional Buck\Boost interleaved converters ($BB_{i,j}$) and the Battery Packs ($BP_{i,j}$) in the OSB sub-system are depicted in Fig. 2. In this figure, the reliability-critical elements, i.e., IGBTs, diodes, capacitors, and battery cells, are marked by red.

B. Operation Analysis

The operational profile of an S2SC system for a short-distanced ferry is usually made up of two recharging scenarios: 1) the opportunity charging while the vessel is loading\unloading and 2) the overnight charging. An example of

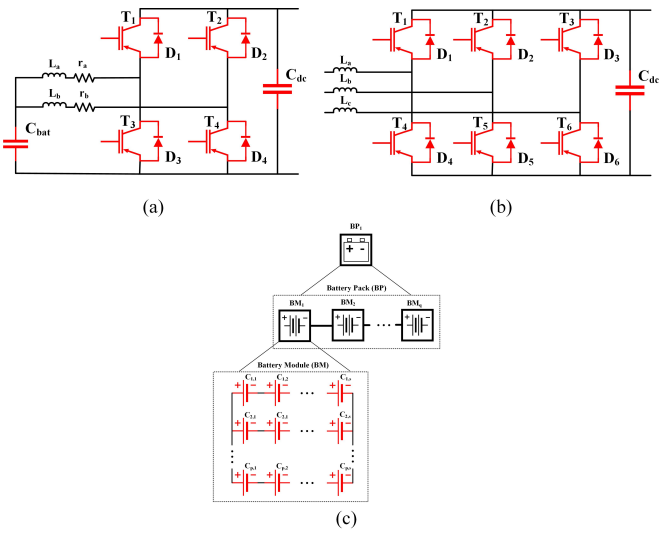

Fig. 2. The schematic of (a) the dc-ac converter ($VSC_{i,j}$), (b) the bidirectional dc-dc converter ($BB_{i,j}$), and (c) the battery pack ($BP_{i,j}$). The critical elements for reliability analysis are colored red.

the operational profile is shown in Fig. 3. Assuming identical transit intervals and charging breaks throughout the day, the operating characteristics of the case study are listed in Table I.

TABLE I
The Case Study Characteristic

Parameter	Value
Number of trips per day (n)	5
Averaged docking time (t_{dock})	25 min
Averaged sailing time between charging ($t_{transit}$)	2 h
Energy consumption in one trip (E_{tr})	1677 kWh
Battery SoC safety range (SoC_{min} – SoC_{max})	15%-90%

In the following, according to the operational profile in Fig. 3, given the constant power during one charging period, the operational analysis of the S2SC system is described. The energy balance of OBBs in 24 hours can be obtained as follows.

$$\begin{aligned}(n-1)[(P_{OSB,dis}+P_G)(t_{OBB,ch1})]\\ +(P_{OBB,ch2})(t_{OBB,ch2})=nE_{tr}\end{aligned} \tag{1}$$

in which $P_{OSB,dis}$ and P_G are the discharging power from OSB and the drawn power from the grid for opportunity charging. Further, $P_{OBB,ch2}$ is the overnight charging power for OBB. The opportunity and overnight charging times are denoted by $t_{OBB,ch1}$ and $t_{OBB,ch2}$. The following constraints must be met:

$$0 \leq t_{OBB,ch1} \leq t_{dock} \tag{2}$$

$$0 \leq t_{OBB,ch2} \leq t_{night} \tag{3}$$

where t_{dock} and t_{night} are the docking time and overnight layover time. The final SoC of the OBB at the end of the last transit, $SoC_{OBB,final}$, can be calculated as follows:

Author Accepted Manuscript version of the paper by Siamak Karimi, Mehdi Zadeh and Jon Are Suul.
in IEEE transactions on industry applications, 59 (2023) Page 4752-4763,
http://dx.doi.org/10.1109/TIA.2023.3258419

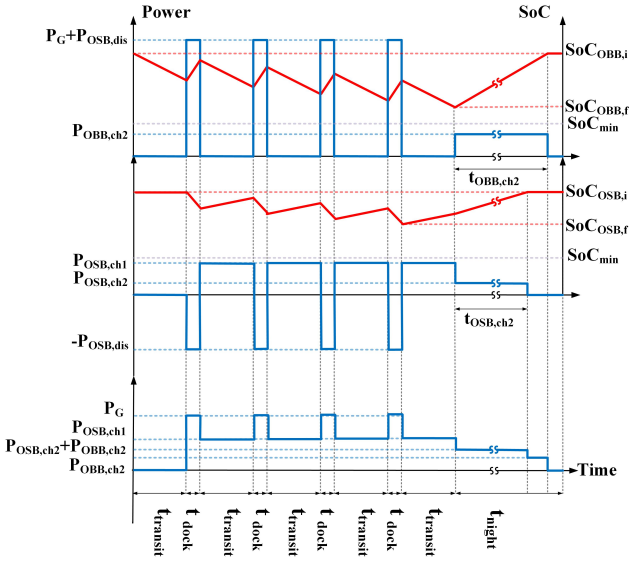

Fig. 3. An example of S2SC operational profile for a short-distanced ferry for 24 hours. From top to bottom, the diagrams depict the power and SoC profile of OBB; the power and SoC profile of OSB; and the grid power. The blue and red profiles are the power and the SoC, respectively.

$$SoC_{OBB,final} = SoC_{OBB,initial} + \frac{1}{C_{OBB}}[-nE_{tr} + (n-1)(P_{OSB,dis} + P_G)(t_{OBB,ch1})] \quad (4)$$

in which C_{OBB} and $SoC_{OBB,initial}$ are the capacity of OBB and its initial SoC as the ship starts operating. The energy balance, the charging time constraints, and the final SoC expression of the OSB can be determined by the same procedure as explained for obtaining (1), (2), (3), and (4) respectively. By so doing, equations (5), (6), (7), and (8) are derived as follows.

$$\begin{aligned}&(n-1)[(P_{OSB,dis})(t_{OBB,ch1})]\\ &= (n-1)(P_{OSB,ch1})(t_{OSB,ch1})\\ &+ (P_{OSB,ch2})(t_{OSB,ch2})\end{aligned} \quad (5)$$

$$0 \leq t_{OSB,ch1} \leq t_{tr} \quad (6)$$

$$0 \leq t_{OSB,ch2} \leq t_{night} \quad (7)$$

$$\begin{aligned}&SoC_{OSB,final} = SoC_{OSB,initial}\\ &+ \frac{1}{C_{OSB}}[-(n-1)(P_{OSB,dis})(t_{OBB,ch1})\\ &+ (n-1)(P_{OSB,ch1})(t_{OBB,ch1})]\end{aligned} \quad (8)$$

in which $P_{OSB,ch1}$, $t_{OSB,ch1}$ and $P_{OSB,ch2}$, $t_{OSB,ch2}$ are the charging power and charging time for daytime charging and overnight charging of OSB.

III. Reliability Analysis

The reliability of an S2SC system is measured by the probability of recharging the onboard batteries with a sufficient amount of energy such that the vessel can operate as planned without any delay or interruption. In the following, a framework for evaluating operation-based reliability of the S2SC system is presented.

From the reliability point of view, the system hierarchy is, from bottom to top, made up of 1) parts, i.e., IGBTs and capacitors, 2) components, such as power converters and battery packs, 3) sub-systems, GI, and OSB and 4) the whole S2SC system. The flowchart illustrating this methodology is shown in Fig. 4. The input variables shown in this flowchart, including the system configuration and operational parameters, were described in the previous section. In the following, the other stages of this flowchart will be explained.

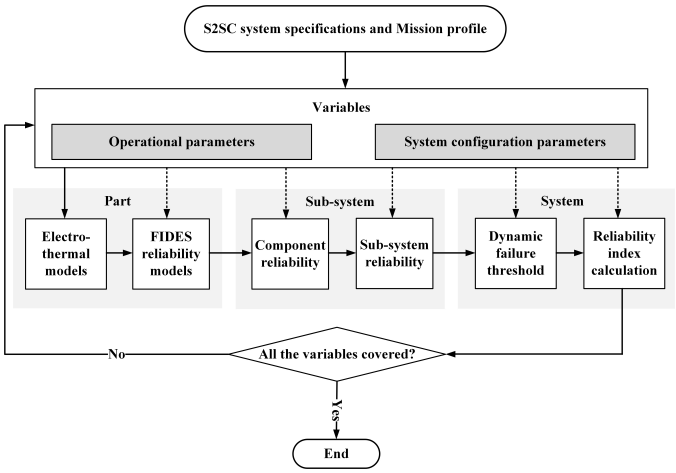

Fig. 4. The operation-based reliability assessment of the S2SC system.

A. Variables

The variables considered in this framework are operational and system configuration parameters. Let $\mathcal{O} := (P_{OBB,ch1}, t_{OBB,ch1}, P_{OBB,ch1}, t_{OBB,ch2}, P_{OSB,ch1}, t_{OSB,ch1}, P_{OSB,ch2}, t_{OSB,ch2})$ denote the operational parameters. Further, let $\mathcal{D} := (N_{GI}, P_{OSB,unit}, N_{GI,unit}, N_{OSB}, C_{OSB}, C_{OBB}, SoC_{min})$ denote the system configuration parameters. In this stage, a range of feasible space is prepared for being assessed by the reliability analysis. In the end, if all the variables are not covered, a new set of variables is chosen for the next iteration. Notably, developing an optimization strategy for finding the optimal set of variables is out of the scope of this paper. However, the presented framework is readily compatible with an optimization problem.

B. Part

To estimate the constant failure during the useful lifetime for the reliability-critical parts of the S2SC system, the FIDES approach is chosen. This approach is selected due to its credibility in applying physics-of-failure-based estimation methods

and suitability for considering the annual mission profile [19]. The failure rate can be calculated as follows:

$$\lambda = \Pi_{PM}\Pi_{Process}\lambda_{Phy} \tag{9}$$

in which Π_{PM} accounts for the effect of the quality and technical control over manufacturing. Further, $\Pi_{Process}$ represents the impact of the processes from specification to field operation and maintenance. To comply with FIDES failure rate estimation, the annual mission profile must be divided into a sequence of phases. Then, the physical contribution to the failure rate, λ_{Phy}, is calculated in each of those phases regarding the thermal, mechanical, and other relevant failure mechanisms associated with the element. The physical contribution to the failure rate can generally be obtained as follows:

$$\lambda_{Phy} = \sum_{i}^{Phases} \frac{t_{annual,i}}{8760}\Pi_i\lambda_i \tag{10}$$

$$\Pi_i = (\Pi_{Placement}\Pi_{App}\Pi_{Rugg})^{0.511\ln(C_{sensitivity})} \tag{11}$$

$$\lambda_i = \sum_{k} \lambda_{0k}\Pi_k \tag{12}$$

in which $t_{annual,i}$ is the duration of the i^{th} phase per year. Further, Π_i denotes the induced electrical, mechanical and thermal overstress factors for each phase which can be calculated based on the instructions in [19]. The failure rate for each phase is called λ_i and is calculated by summing up the component-specific base failure rates, λ_{0k}, multiplied by their correspondent acceleration factors, Π_k. Such acceleration factors and base failure rates are dependent on the design aspects, case types, temperature, humidity, and mechanical stress during each phase. Note that the dormant phases are also considered in this method. In order to obtain the temperature profile required to calculate these acceleration factors, the electrothermal models of the parts, as described in [13], are used. The detailed failure rate models can be found in [19].

C. Sub-system

While the failure rates of the parts are calculated by the FIDES approach, the failure rates of components are directly obtained by using the series reliability block diagram approach [28]. Then, for each sub-system, the Markov chain is drawn as a set of components connected in series. As a result, the probability of various operation states with their capacity is calculated [13].

Given that the sub-systems are made up of several parallel units, any unit failure can lead to a reduced power capacity of the sub-system. The reduced capacity of sub-system x, $x \in \{GI, OSB\}$, with N_x units in parallel, when k out of N_x units are still operating normally, is calculated a :

$$Cap_x(k) = kP_{x,unit} \quad k = 0, 1, 2, ..., N_x \tag{13}$$

where $P_{x,unit}$ is the nominal power capacity of one unit in the sub-system x. Ultimately, the probability-capacity table of the sub-systems is calculated. Moreover, $\mathcal{R}_x$ is defined as a set containing the probability, $Pr_x(k)$, and capacity, $Cap_x(k)$, of the sub-system x.

D. System

Thus far, the capacity table of the whole system is obtained as $\{Pr_{sys}, Cap_{sys}\}$. To evaluate the system reliability, LOLE, which is a conventional index designated for the power system, can be used.

$$LOLE = 365\sum_{i=1}^{m} Pr_{sys}(i)T(i) \tag{14}$$

where m indicates the number of capacity states of the whole system. Furthermore, $T(i)$ is determined based on the load duration curve and indicates the time duration during which the demanded load is $Cap_{sys}(i)$ [28]. However, these indices might not be the best benchmarking factors for assessing the reliability of the studied S2SC systems since the derivation of the load duration curve can be complex. The challenges are especially caused by the low utilization ratio of S2SC systems combined with marginal flexibility of the charging loads and the energy balance requirements of the batteries. Additionally, the de-rated operation cannot be measured by the conventional power system reliability indices. To interpret the calculated system reliability capacity probability tables into their impacts on the S2SC performance and the ship transits, application-specific reliability indices are preferred. Such reliability indices are defined in [7]. The first index is the Loss of Charging Expected (LOCE) which indicates the expected number of failed charging breaks per year and is defined as follows:

$$LOCE = \sum_{i=1}^{365}\sum_{j=1}^{n} Pr(f) \tag{15}$$

where $Pr(f)$ represents the probability of the final failure of the whole system. The other S2SC-specific reliability index is Derated Charging Expected (DCE) which estimated the number of derated charging breaks per year and is calculated by the following expression.

$$DCE = \sum_{i=1}^{365}\sum_{j=1}^{n} Pr(d) \tag{16}$$

where $Pr(d)$ represents the probability of the derated charging occurrence. Note that the yearly mission profile of the ship is taken into account to obtain such indices. To calculate $Pr(f)$ and $Pr(d)$, a dynamic failure threshold approach is taken into account. In reliability studies, constructing a failure threshold is necessary in order to categorize the operation states into different classes: normal, derated and the final failure [28]. For S2SC systems, since the loads are OBBs, a reduction in transmitted charging energy can cause the final SoC of OBB to fall below its nominal value. Nevertheless, given the safety boundary defined for the OBB SoC, in case of a derated S2SC, the vessel can continue transiting as long as the OBB SoC is within the allowable range. Consequently, higher overnight

Author Accepted Manuscript version of the paper by Siamak Karimi, Mehdi Zadeh and Jon Are Suul.
in IEEE transactions on industry applications, 59 (2023) Page 4752-4763,
http://dx.doi.org/10.1109/TIA.2023.3258419

OBB charging power is required to top up the relatively deeply discharged batteries for the next day [7]. That being said, a dynamic failure threshold is needed to sufficiently capture the performance of the S2SC system. Here, the dynamic failure threshold approach is illustrated via algorithm 1.

Algorithm 1 Calculation of S2SC-specific reliability indices by the dynamic failure threshold.

Input: $\mathcal{R}_{GI}, \mathcal{R}_{OSB}, \mathcal{O}$ and $\mathcal{D}$.
Output: $LOCE$ and DCE.

Initialisation : $Pr(f) = 0$ and $Pr(d) = 0$.
for $u = 1$ to N_{GI} **do**
  for $v = 1$ to N_{OSB} **do**
    $P^*_G = min(Cap_{GI}(u), P_G)$.
    $P^*_{OSB,dis} = min(Cap_{OSB}(v), P_{OSB,dis})$.
    $P^*_{OSB,ch1} = min(Cap_{OSB}(v), Cap_{GI}(u), P_{OSB,ch1})$
    $P^*_{OSB,ch2} = min(Cap_{OSB}(v), Cap_{GI}(u), P_{OSB,ch2})$
    Compute $SoC^*_{OBB,final}$ by (4).
    Compute $SoC^*_{OSB,final}$ by (8).
    if $(SoC^*_{OBB,final} < SoC_{min})$ **or** $(SoC^*_{OSB,final} < SoC_{min})$ **then**
      $Pr(f) = Pr(f) + Pr_{GI}(u).Pr_{OSB}(v)$
    else if $(SoC^*_{OBB,final} < SoC_{OBB,final})$ **or** $(SoC^*_{OSB,final} < SoC_{OBB,final})$ **then**
      $Pr(d) = Pr(d) + Pr_{GI}(u).Pr_{OSB}(v)$
    end if
  end for
end for
Compute $LOCE$ by (15).
Compute DCE by (16).
return $LOCE$ and DCE.

In this algorithm, the threshold operating parameters, such as P^*_G, are calculated based on the failure-driven reduced capacity of the sub-systems and actual operation parameters extracted from $\mathcal{O}$. Such thresholds substitute the actual values in the 4 and 6, to obtain $SoC^*_{OSB,final}$ and $SoC^*_{OBB,final}$. If at least one of these SoC values is lower than the safety limit, SoC_{min}, the vessel operation is failed. Furthermore, if at least one of the final SoC values is lower than their nominal values, yet higher than the safety limit, the S2SC operation is defined as derated. Otherwise, the S2SC operation attributed to the applied number of failed units is defined as normal.

Note that, the operation modes, i.e., normal, derated, and failed, are dependant on $\mathcal{R}_{GI}$, $\mathcal{R}_{OSB}$, and $\mathcal{O}$. The obtained failure thresholds are depicted for two different sets of operational variables in Fig. 5 (a) and (b). It is obvious that by posing different operating scenarios, the definition of derated and failed states can be altered.

IV. Battery Lifetime Estimation

To model the battery lifetime, an experimentally-verified aging model is used. This model considers the calendar and cycling factors for capturing the capacity fade effect of NMC Li-ion battery cells [26]. To calculate the lifetime of the battery cells, it takes into account the cell temperature, cell voltage, cycle depth, and SoC range. The aging model is defined by the following expressions [26]:

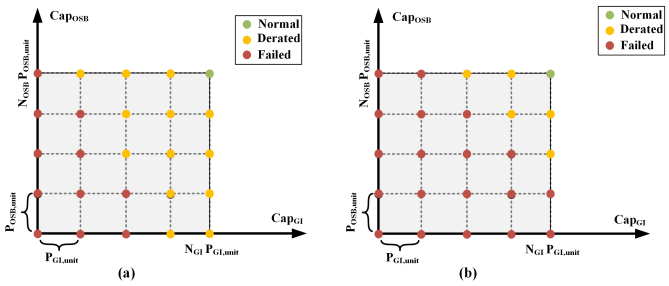

Fig. 5. An example showing that the failure consequences determined by the dynamic failure threshold might be different for each set of operational parameters ($\mathcal{O}$).

$$C = 1 - \alpha_{cal}.t^{0.75} - \alpha_{cyc}.\sqrt{Q} \tag{17}$$

$$\alpha_{cal} = (7.543V - 23.75).10^6 e^{\frac{-6976}{T}} \tag{18}$$

$$\begin{aligned}\alpha_{cyc} =& 7.348.10^{-3}.(V_{avg} - 3.667)^2 + 7.6.10^{-4} \\ &+ 4.081.10^{-3}\Delta DoD\end{aligned} \tag{19}$$

where C denotes the ratio of actual capacity to its initial value and is less than one. When C is reduced to 0.8, the battery has reached its end of life. Further, v, T, V_{avg}, ΔDoD and Q are the storage cell voltage in V, cell temperature in K, the averaged cell voltage in V, the depth of discharge and the charge throughput in $A.h$. Moreover, t denotes the number of days.

V. Results and Discussion

In this section, the case study is first described. Then, using the FIDES approach, the failure rates of the critical parts are estimated and compared to the ones calculated by the MIL-HDBK-217F models. Then, the system-level reliability using the method introduced in section III is applied. Furthermore, a selected range of OSB power profile scenarios is formulated by means of two ratios and tested in terms of reliability. In the end, the SoC energy profile scenarios are tested with regard to the onshore battery lifetime. Accordingly, a few suggestions for OSB power and energy profile planning are given. It is worth mentioning that in order to simplify the analysis, only a certain range of feasible scenarios based on the practical constraints are chosen for the case study. However, the framework is compatible with utilization for evaluating a vast range of scenarios and alternatives from the reliability point of view.

A. Failure rates and reliability indices for the case study

In addition to the operational characteristics of the case study as shown in Table I, the operational parameters used in equations (1)-(8) are listed in Table II. The IGBT module considered for the dc-dc and ac-dc converters is FF1500R17IP5P [29]. More detailed design parameters of power electronics converters can be found in [13].

Author Accepted Manuscript version of the paper by Siamak Karimi, Mehdi Zadeh and Jon Are Suul.
in IEEE transactions on industry applications, 59 (2023) Page 4752-4763,
http://dx.doi.org/10.1109/TIA.2023.3258419

TABLE II
THE OPERATIONAL PARAMETERS

Parameter	Value
$P_{OSB,dis}$	2MW
$P_{OBB,ch1}$, $t_{OBB,ch1}$	4 MW, 25 min
$P_{OBB,ch2}$, $t_{OBB,ch2}$	0.4 MW, 196 min
$P_{OSB,ch1}$, $t_{OSB,ch1}$	0.4 MW, 2 h
$P_{OSB,ch2}$, $t_{OSB,ch2}$	0.1 MW, 8 h

As described in section III, the operational profile must be categorized into different phases to calculate the failure rates. Regarding the operational profile depicted in Fig. 3, the following phases can be defined. 1) transit, 2) docking, 3) OBB overnight charging and 4) OSB overnight charging. Subsequently, the thermal profile is derived according to the power and duration of such phases by means of the electrothermal models. Note that to calculate the failure rate of the battery packs, based on the FIDES approach, two types of failure rates are calculated: 1) the cell-based constant failure rate which is estimated based on the equation (9), and 2) wear-out failure rate which is dependent on the lifetime of the battery [23]. The detailed values for part failure rates are extracted from [19].

The calculated failure rates for the parts are listed in table III. Further, the failure rates of the parts and components are shown in Fig. 6.

TABLE III
CALCULATED FAILURE RATES OF THE PARTS.

Part name	FIDES failure rate (in FIT)	MIL-HDBK-127 failure rate (in FIT)
Batteries		
Battery cells	26 (4110)[a]	200
dc-dc converter		
IGBT	255	979
Diode	121	123
dc-bus capacitor	59	210
Battery-side capacitor	48	199
ac-dc converter		
IGBT	139	812
Diode	47	89
dc-bus capacitor	58	351

[a]It refers to the wear-out term which is estimated for the battery pack.

As is obvious from table III, the FIDES reliability approach estimates the failures more optimistically since it takes into account the operation profile rather than the worst-case operation point to calculate the failure rates. In this case, the worst-case operating point occurs only approximately 2.5 hours per day, during the regular opportunity charging of the ferry. Therefore, the FIDES-based failure rates are significantly lower than those calculated based on the assumption that the system always performs on the worst-case operating point. Similar results regarding the comparison between these two reliability handbooks are observed in [17].

It can be concluded from Fig. 6 (a) that the IGBTs have the highest failure rates in both power converters. In the component-level comparison, it can be observed from Fig. 6 (b) that the battery packs are much more prone to failure

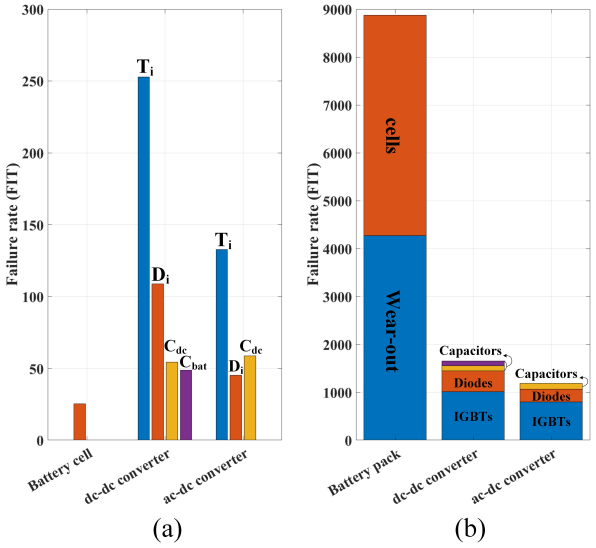

Fig. 6. The estimated failure rates based on the FIDES handbook for (a) the parts and (b) the components.

compared to the dc-dc and ac-dc converters. To calculate the failure rate of the capacitors by FIDES, the main factors are the ratio of the applied voltage to the rated voltage as well as the thermal cycling [19]. In fact, the higher the number of parallel capacitors, complying with the required capacitance, the less thermal stress is posed on each capacitor. However, by increasing the number of parallel capacitors, the equivalent failure rate increases. Furthermore, the capacitors are chosen such that their voltage stress factor is less than 0.5, thereby minimizing their failure rate.

In the next stage, applying the reliability assessment method depicted in Fig. 4, the reliability indices are calculated and listed in Table IV. The obtained results are compared with the indices calculated by the reliability framework presented in [13]. Notably, to compare the results, the modified case study in this work is applied to the design framework in [13].

TABLE IV
THE CALCULATED RELIABILITY INDICES.

Index	LOLE	LOCE	DCE
This framework	0.32 d/y[a]	1.46 CB/y[b]	31.93 CB/y
Framework in [13]	0.41 d/y	2.80 CB/y	16.49 CB/y

[a]Charging Breaks per year.
[b]days per year.

As it is shown in Table IV, according to the operation-based framework, it is expected that the S2SC system fails to supply the demanded charging load for 0.32 days per year. Furthermore, 1.46 and 31.93 charging breaks per year are stopped and derated, respectively, due to failures. In comparison, the reliability framework in [13] which is based on MIL-HDBK-217F models estimates 0.41 days of lost load in a year and it predicts that 2.80 and 16.49 charging breaks per year are stopped and derated. It can be seen that the operation-based reliability assessment proposed in this paper, estimates the lost and failed S2SC more optimistically than that obtained

Author Accepted Manuscript version of the paper by Siamak Karimi, Mehdi Zadeh and Jon Are Suul.
in IEEE transactions on industry applications, 59 (2023) Page 4752-4763,
http://dx.doi.org/10.1109/TIA.2023.3258419

by the design-based framework due to the utilization of the FIDES approach. Moreover, it can be seen that the estimation of derated S2SC is higher in the operation-based framework. It is a consequence of using the dynamic failure threshold, which considers the OSB and OBB energy balances to investigate the derated operation states. Therefore, more derated states are identified in the operation-based framework compared to the design framework in [13].

Another aspect that can be compared to the other framework is the computational effort. The computer programs have been run in MATLAB on a personal computer with Intel(R) Core(TM) i7-8665U CPU @ 1.9 GHz and 16 GB memory. Time elapsed for one iteration, with one set of operational parameters, is 1.36 seconds. While the elapsed time for running the design framework in [13] is 1.09 seconds. Hence, it can be concluded that conducting the operation-based framework does not impose any big limitations on practical use.

B. Impact of OSB scheduling on the reliability

In this section, the effect of operational planning in terms of OSB scheduling on the reliability indices is investigated. The selected operational parameters include the load-sharing between the grid and OSB during the OBB charging intervals, the recharging interval of the OSB between the trips, and the overnight charging of the OSB. To derive the feasible operational scenario space, for being tested by the framework, the following remarks and assumptions are considered.

1) This analysis is carried out for the same sizing of the S2SC system and route schedule of the vessel. It also means that the requested charging energy and power by the ship is assumed to be constant.
2) The load-sharing ratio between the OSB and grid is considered to remain constant for all the vessel charging intervals.
3) The power drawn from the grid to recharge the OSB, $P_{OSB-dis}$, is not higher than that to charge the OBB charging, P_G.
4) The OSB recharging time is calculated as $min(t_{tr}, \frac{P_{OSB-dis} t_{OBB-ch1}}{P_{OSB-ch1}})$. It means that the OSB recharging interval cannot be longer than the time between two transits. In order to validate the feasibility of a set of power set-points for OSB, the final SoC of the OSB after the last OBB charging interval is checked to not be lower than the SoC minimum limit.

To quantify the OSB scheduling scenarios considering the aforementioned constraints and conditions, two ratios are defined as follows:

1) $\frac{P_G}{P_{OBB-ch1}}$: It is called Grid Power Ratio (GPR) which accounts for the load sharing between the grid and OSB.
2) $\frac{P_{OSB-ch1}}{P_G}$: It refers to the ratio of the recharging power of the OSB between the trips over the grid power for the OBB charging.

Here, these ratios are called OSB scheduling ratios. To show the impact of such operational parameters, three examples with different OSB scheduling ratios are chosen and their associated LOCE and DCE indices are calculated. The results are presented in Table V.

TABLE V
THREE EXAMPLES OF OSB SCHEDULING

Parameter	$\frac{P_G}{P_{OBB-ch1}}$	$\frac{P_{OSB-ch1}}{P_G}$	$P_{OSB,dis}$	$P_{OSB,ch1}$	LOCE	DCE
Scenario 1	0.54	0.4	$1.84MW$	$0.86MW$	1.46	30.93
Scenario 2	0.75	0.05	$1MW$	$0.15MW$	1.46	36.79
Scenario 3	0.84	0.25	$0.64MW$	$0.84MW$	1.52	32.32

As it can be seen from comparing the reliability indices for the three examples, the expected number of the charging breaks being lost due to failures is the highest for scenario 3, although the difference between the calculated LOCE values is insignificant. Furthermore, the expected derated charging intervals are largest for scenario 2 in which 25% of the OBB charging power is supplied by the OSB, and OSB is charged by 150 kW between the trips.

By applying the operation-based reliability framework for a certain range of the OSB scheduling ratios, the trends for LOCE and DCE are drawn in Fig. 7. The defined scenario examples in Table V are also shown in Fig. 7. As can be seen in Fig. 7 (a), the sensitivity of the LOCE to the y-axis is mostly higher than that to the x-axis, for the applied range of OSB scheduling ratios. It is because of the fact that the grid power ratio determines the DoD of the OSB for charging the OBB. Moreover, as shown in Fig. 7 (a), the change of the LOCE is insignificant for a grid power ratio less than 0.8. However, for $0.8 < \frac{P_G}{P_{OBB-ch1}} < 0.9$ the LOCE decreases by increasing OSB discharging power.

Regarding the expected derated charging breaks, as shown in Fig. 7 (b), it can be seen that the trend of DCE shows its minimum in the vicinity of $\frac{P_G}{P_{OBB-ch1}} = 0.65$ and $\frac{P_{OSB-ch1}}{P_G} = 0.45$. This can be explained by the transition from higher OSB power and shorter time under operation to lower OSB power and longer time under operation, which occurs by decreasing the grid power ratio. For instance, it is obvious from Fig. 7 (b) that the lowest DCE, which is 31.41 CB per year, occurs for $0.52 < \frac{P_G}{P_{OBB-ch1}} < 0.78$ and $\frac{P_{OSB-ch1}}{P_G} = 0.5$.

Moreover, based on the DCE trend, the very high and very low grid power ratios result in more derated charging breaks expected due the high loading of the GI and OSB units, respectively. For example, as seen for scenario 2, increasing the recharging power ratio from 0.05 to 0.15 results in the number of expected de-rated charging breaks being reduced by more than 5 CB/year. Thus, incorporating such trends into the planning tools can result in a significant improvement in the system's reliability performance.

Next, the impact of the overnight charging power for the OSB on reliability is investigated. To this end, by applying $\frac{P_G}{P_{OBB-ch1}} = 0.5$ and $\frac{P_{OSB-ch1}}{P_G} = 0.25$, the reliability indices with regards to the overnight charging power are shown in Fig. 8.

According to Fig. 8 (a), it can be concluded that the increase in the OSB night charging power can slightly improve reliability. As it is obvious from Fig. 8 (b), the increase of OSB night charging power by four times, from 100 kW to 400 kW can decrease the DCE by approximately 7 CB/yr. However, the change of LOCE and DCE per one charging

Author Accepted Manuscript version of the paper by Siamak Karimi, Mehdi Zadeh and Jon Are Suul.
in IEEE transactions on industry applications, 59 (2023) Page 4752-4763,
http://dx.doi.org/10.1109/TIA.2023.3258419

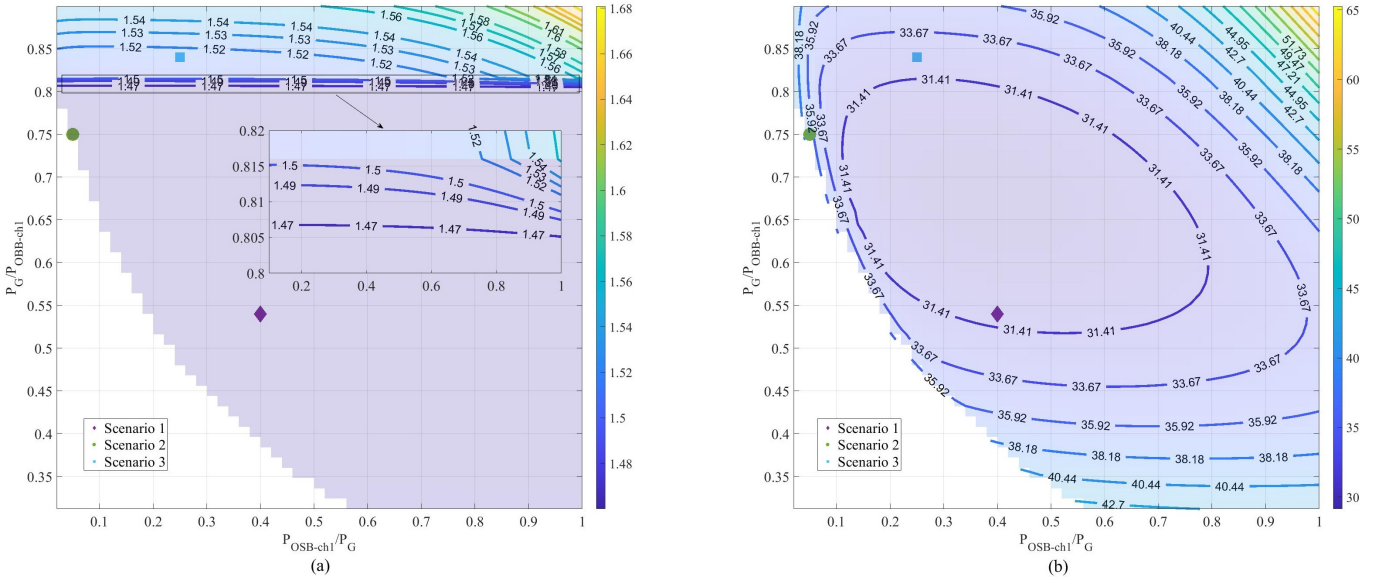

Fig. 7. The (a) LOCE and (b) DCE obtained for the different OSB scheduling scenarios.

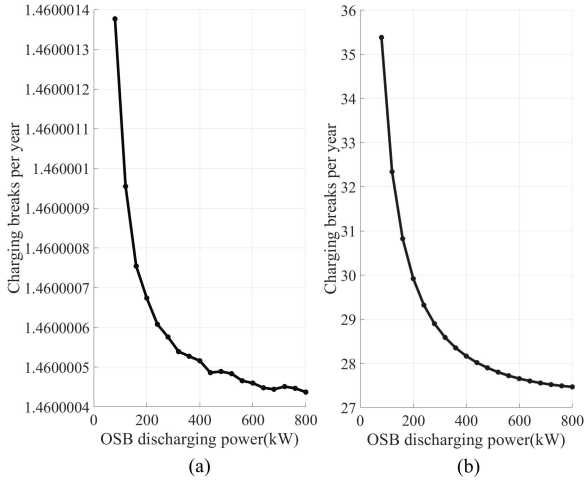

Fig. 8. The (a) LOCE, and (b) DCE for OSB night charging.

power step decreases as the charging power increases. It is worth mentioning that the same trend for the reliability indices in terms of the night charging power is observed for the other OSB scheduling ratios. It can be explained by the fact that by increasing the overnight slow charging power, the reduction of the overnight charging duration can lead to higher reliability.

Notably, if MIL-HDBK-217F reliability models are used, the predicted reliability would be constant for most of the aforementioned operational parameter ranges. It is because the worst-case operating points are kept similar, although their duration might alter.

C. Impact of OSB scheduling on the battery lifetime

In addition to the charging and discharging power set-points, the energy profile or SoC profile of the batteries are determined in the operation planning phase. However, the FIDES battery reliability model does not directly take into account the SoC profile. Therefore, the battery lifetime prediction model is used as a complementary approach to assess the SoC profile candidates. To formulate the SoC profiles being swept for the lifetime analysis, the OSB scheduling ratios, initial SoC value, and battery capacity are considered. To carry out the analysis in a more simplified way, only three initial SoC values, 0.7, 0.8, and 0.9, and two battery capacity values, 2MWh and 3MWh, are chosen. The aforementioned scenarios are numbered in Table VI, and their associated SoC profiles are drawn in Fig. 9.

TABLE VI
THE SCENARIOS NUMBERS WITH DIFFERENT OSB SCHEDULING RATIOS, BATTERY CAPACITIES, AND INITIAL SOC VALUES

$SoC_{OSB-initial}$	0.9		0.8		0.7	
C_{OSB}	$2MWh$	$3MWh$	$2MWh$	$3MWh$	$2MWh$	$3MWh$
Scenario 1	1.1	1.2	1.3	1.4	1.5	1.6
Scenario 2	2.1	2.2	2.3	2.4	2.5	2.6
Scenario 3	3.1	3.2	3.3	3.4	3.5	3.6

As can be seen in Fig. 9, the scenarios with different battery capacities and initial SoC values can lead to different SoC profiles. Notably, scenario 2.5 would not be feasible since its final value violates the SoC minimum limit.

Note that such an aging model is used to benchmark the operational scenarios. Moreover, the predicted lifetime results are highly dependent on the experimental measurements on a specific battery cell used in [26]. Using this model, the battery lifetime regarding the 18 scenarios introduced in Table VI is estimated and listed in Table VII.

TABLE VII
THE ESTIMATED NUMBER OF DAYS IN OPERATION FOR THE BATTERY IN THE OSB FOR THE DIFFERENT SCENARIOS

$SoC_{OSB-initial}$	0.9		0.8		0.7	
C_{OSB}	$2MWh$	$3MWh$	$2MWh$	$3MWh$	$2MWh$	$3MWh$
Scenario 1	513	957	597	1172	663	1367
Scenario 2	787	1458	870	1710	-	1917
Scenario 3	1852	2633	2388	3401	2967	4256

Author Accepted Manuscript version of the paper by Siamak Karimi, Mehdi Zadeh and Jon Are Suul.
in IEEE transactions on industry applications, 59 (2023) Page 4752-4763,
http://dx.doi.org/10.1109/TIA.2023.3258419

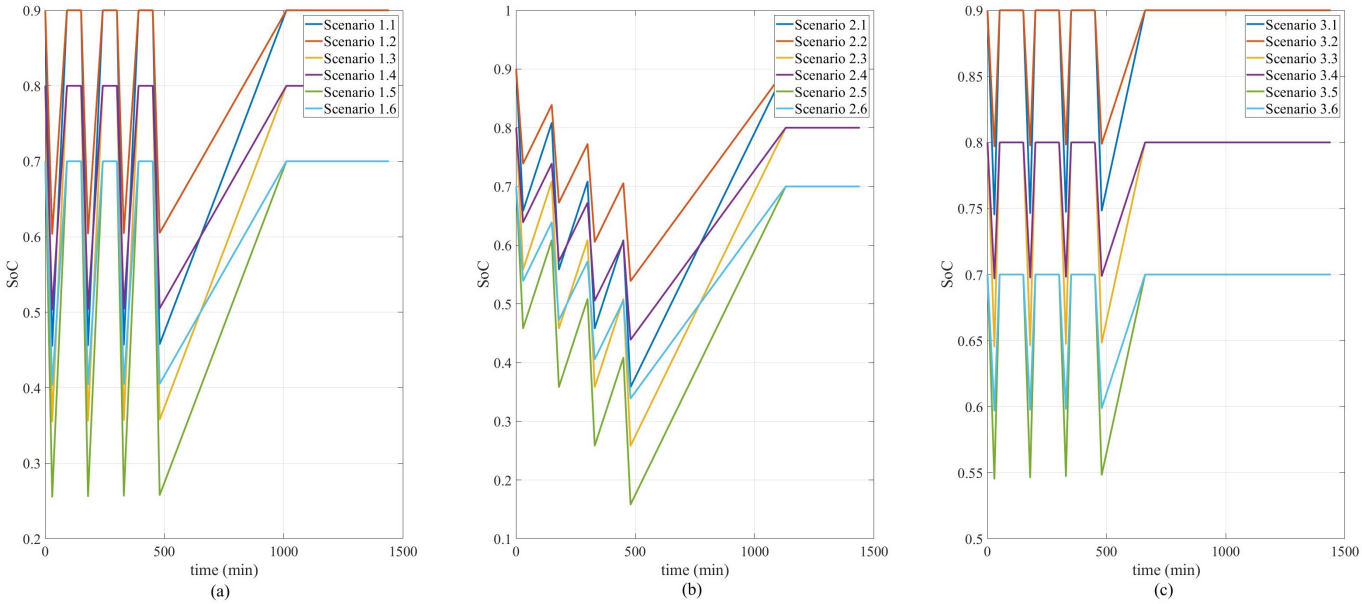

Fig. 9. The SoC profile of the (a) scenario group 1, (b) scenario group 2, and (c) scenario group 3.

It can be concluded from the results in Table VII that an increase in the capacity of the batteries in the OSB can significantly improve the lifetime of the battery. For example, by comparing scenarios 2.1 and 2.2 with 22% DoD of the OSB, it can be seen that the lifetime is approximately doubled by increasing the battery capacity by 50%. Moreover, considering scenarios 2.2, 2.4, and 2.6, it is obvious that for the lower initial SoC values the estimated lifetime is longer. It is because the SoC profiles with the SoC cycle range in the vicinity of the 50-60% SoC result in longer battery lifetime compared to cycling around very high or low SoC values [26]. Thus, for a grid power ratio of 0.75, the lifetime of the battery can be extended by approximately 2.5 times by adjusting the SoC cycling range and increasing the battery size by 50%. Further, regarding scenarios 3.1 and 3.5, it can be concluded that modifying the initial SoC value from 90% to 70% can lead to a 60% extension in the battery lifetime.

To better illustrate the impact of influencing factors on the battery lifetime, the predicted lifetime in terms of the number of days in operation for a certain range of OSB scheduling ratios is drawn in Fig. 10 and Fig. 11. The selected scenario examples are also shown in these figures.

Considering the lifetime trend shown in Fig. 10 and Fig. 11, it can be concluded that among the studied influence factors the recharging power of the OSB has the least impact on the lifetime. However, it is obvious that for higher OSB discharging power shorter lifetime is expected. Additionally, larger battery capacity and lower initial SoC value – provided that it shifts the average cycling SoC closer to the middle of the SoC profile – lead to an extended lifetime. Thus, these results can help to design and plan for the battery sizing considering the other operational influence factors.

Conclusion

In this work, a framework for operation-based reliability assessment of S2SC systems by using the FIDES method was proposed. To determine the consequences of the component failure on the S2SC functionality, a dynamic failure threshold was introduced. The presented approach can be utilized for finding the most suitable operation scenarios from a reliability point of view. Additionally, the battery lifetime model, as a complementary approach to reliability, has been employed to benchmark the SoC profile characteristics of the batteries in the OSB sub-system.

The results showed that the estimated failure rates obtained by FIDES are more optimistic than those calculated by MIL-HDBK-217F reliability models, thanks to the capability of FIDES for taking into account the mission profile and physics of failure mechanisms. A set of modified reliability indices are calculated for a certain range of the load-sharing ratio between the OSB and the grid, the OSB recharging power, and the overnight OSB recharging power. On this basis, relevant recommendations on how operational planning can result in reliability improvement can be obtained. For instance, it was shown that an increase in overnight charging power can improve reliability. In the end, it was concluded that for a specific OSB power profile, a lower initial SoC value–while the cycling average value of the SoC is closer to 50%–can result in an extended battery lifetime.

The presented framework could be used to establish a mixed integer nonlinear programming optimization problem to identify the optimal OSB dispatching for certain load demands and design space. Additionally, this model is compatible with the ship profile to realize a reliability-aware charging and transit profile allocation for plug-in battery-electric marine vessels.

References

[1] E. Skjong, R. Volden, E. Rødskar, M. Molinas, T. A. Johansen, and J. Cunningham, “Past, present, and future challenges of the marine

Author Accepted Manuscript version of the paper by Siamak Karimi, Mehdi Zadeh and Jon Are Suul.
in IEEE transactions on industry applications, 59 (2023) Page 4752-4763,
http://dx.doi.org/10.1109/TIA.2023.3258419

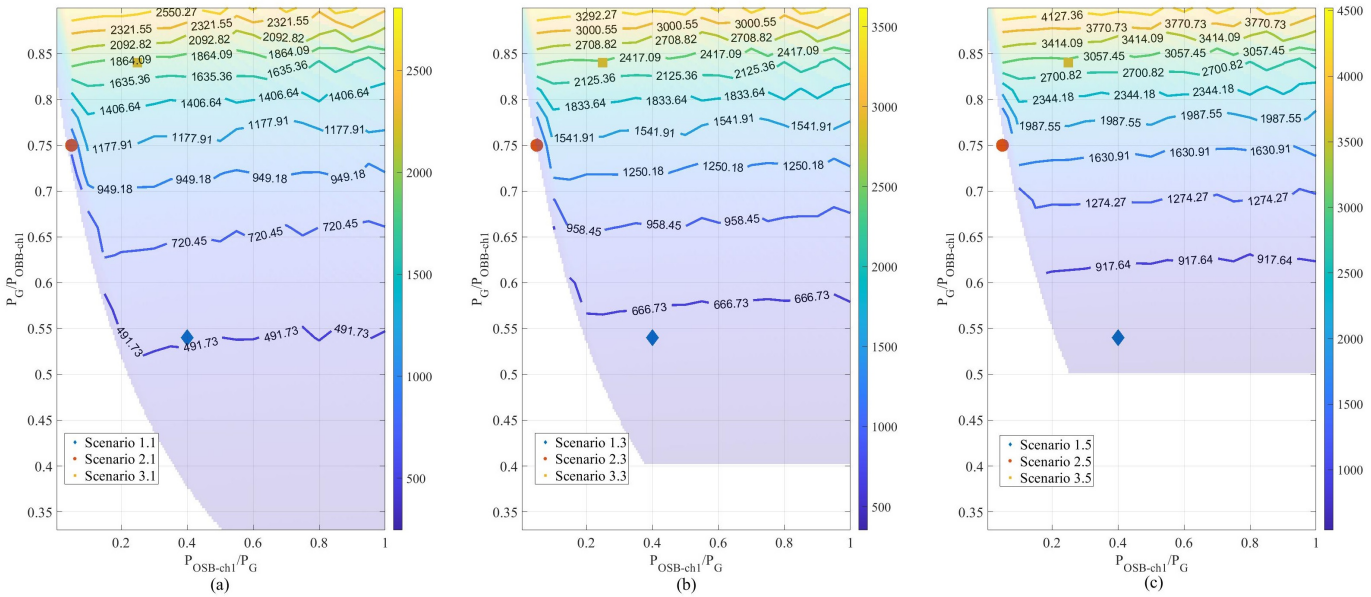

Fig. 10. The calculated lifetime for the initial SoC of (a) 90%,(a) 80% and (a) 70% for the battery size of $2MWh$.

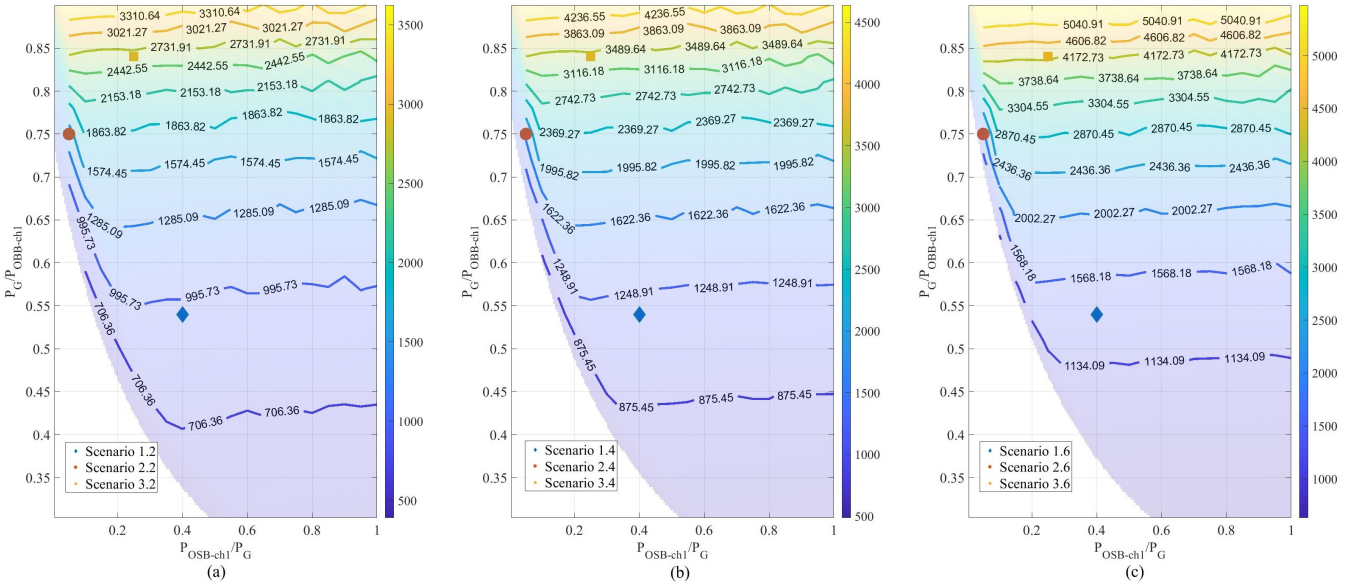

Fig. 11. The calculated lifetime for the initial SoC of (a) 90%,(a) 80% and (a) 70% for the battery size of $3MWh$.

vessel's electrical power system," *IEEE Transactions on Transportation Electrification*, vol. 2, no. 4, pp. 522–537, 2016.

[2] T. Ericsen, N. Hingorani, and Y. Khersonsky, "Power electronics and future marine electrical systems," *IEEE transactions on industry applications*, vol. 42, no. 1, pp. 155–163, 2006.

[3] S. Karimi, M. Zadeh, and J. Suul, "Evaluation of energy transfer efficiency for shore-to-ship fast charging systems," in *2020 IEEE 29th International Symposium on Industrial Electronics (ISIE)*, Delft, Netherlands, 2020.

[4] DNV-Maritime, "Alternative fuel insights (AFI)." [Online]. Available: https://afi.dnvgl.com

[5] S. Karimi, M. Zadeh, and J. Suul, "Shore charging for plug-in battery-powered ships: Power system architecture, infrastructure, and control," *IEEE Electrification Magazine*, vol. 8, no. 3, p. 47–61, 2020.

[6] V. P. Lavall, "Regulation (eu) no 1177/2010 and protection of passengers in sea and inland waterway transport," *EJCCL*, vol. 5, p. 65, 2013.

[7] S. Karimi, M. Zadeh, and J. Suul, "Reliability analysis of shore-to-ship fast charging systems," in *2021 IEEE Transportation Electrification Conference & Expo (ITEC*, Chicago, US, 2021.

[8] J. Guo, X. Wang, J. Liang, H. Pang, and J. Gonçalves, "Reliability modeling and evaluation of MMCs under different redundancy schemes," *IEEE Transactions on Power Delivery*, vol. 33, no. 5, p. 2087–2096, 2018.

[9] P. Tu, S. Yang, and P. Wang, "Reliability- and cost-based redundancy design for modular multilevel converter," *IEEE Transactions on Industrial Electronics*, vol. 66, no. 3, p. 2333–2342, 2019.

[10] X. Yu and A. Khambadkone, "Reliability analysis and cost optimization of parallel-inverter system," *IEEE Transactions on Industrial Electronics*, vol. 59, no. 10, p. 3881–3889, 2012.

[11] M. Rausand, *Reliability of safety-critical systems: theory and applications*. John Wiley & Sons, 2014.

[12] R. N. Allan *et al.*, *Reliability evaluation of power systems*. Springer Science & Business Media, 2013.

[13] S. Karimi, Z. M, and J. Suul, "A multi-layer framework for reliability assessment of shore-to-ship fast charging system designs," *IEEE Transactions on Transportation Electrificaiton*, 2021.

Author Accepted Manuscript version of the paper by Siamak Karimi, Mehdi Zadeh and Jon Are Suul.
in IEEE transactions on industry applications, 59 (2023) Page 4752-4763,
http://dx.doi.org/10.1109/TIA.2023.3258419

[14] Y. Song and B. Wang, "Survey on reliability of power electronic systems," *IEEE transactions on power electronics*, vol. 28, no. 1, pp. 591–604, 2012.
[15] Y. Yang, H. Wang, A. Sangwongwanich, and F. Blaabjerg, "Design for reliability of power electronic systems," in *Power electronics handbook*. Elsevier, 2018, pp. 1423–1440.
[16] M. Liu, W. Li, C. Wang, M. P. Polis, J. Li *et al.*, "Reliability evaluation of large scale battery energy storage systems," *IEEE Transactions on Smart Grid*, vol. 8, no. 6, pp. 2733–2743, 2016.
[17] P. I. Prodanov and D. D. Dankov, "Comparison of failure rates and reliability of power semiconductors in power electronic devices using methodologies MIL-HDBK-217F and FIDES," in *2021 17th Conference on Electrical Machines, Drives and Power Systems (ELMA)*. IEEE, 2021, pp. 1–5.
[18] S. Peyghami, Z. Wang, and F. Blaabjerg, "A guideline for reliability prediction in power electronic converters," *IEEE Transactions on Power Electronics*, vol. 35, no. 10, p. 10958–10968, 2020.
[19] FIDES Group and others, "Fides guide 2009 edition a-reliability methodology for electronic systems," *AIRBUS France, Eurocopter, Nexter Electronics, MBDA missile systems, Thales Systèmes Aéroportés SA, Thales Avionics, Thales Corporate Services SAS, Thales Underwater Systems*, 2014.
[20] K. Smith, A. Saxon, M. Keyser, B. Lundstrom, Z. Cao, and A. Roc, "Life prediction model for grid-connected Li-ion battery energy storage system," in *2017 American Control Conference (ACC)*. IEEE, 2017, pp. 4062–4068.
[21] S. Peyghami, H. Wang, P. Davari, and F. Blaabjerg, "Mission-profile-based system-level reliability analysis in dc microgrids," *IEEE Transactions on Industry Applications*, vol. 55, no. 5, p. 5055–5067, 2019.
[22] S. Peyghami, P. Davari, and F. Blaabjerg, "System-level reliability-oriented power sharing strategy for dc power systems," *IEEE Transactions on Industry Applications*, vol. 55, no. 5, p. 4865–4875, 2019.
[23] V. Raveendran, M. Andresen, and M. Liserre, "Improving onboard converter reliability for more electric aircraft with lifetime-based control," *IEEE Transactions on Industrial Electronics*, vol. 66, no. 7, p. 5787–5796, 2019.
[24] J. Jiang, S. Peyghami, C. Coates, and F. Blaabjerg, "A comprehensive study on reliability performance of photovoltaic-battery-based microgrids under different energy management strategies," *Journal of Energy Storage*, vol. 43, p. 103051, 2021.
[25] S. Karimi, M. Zadeh, and J. A. Suul, "Operation-based reliability assessment of shore-to-ship charging systems," in *2022 IEEE/IAS 58th Industrial and Commercial Power Systems Technical Conference (I&CPS)*. IEEE, 2022, pp. 1–7.
[26] J. Schmalstieg, S. Käbitz, M. Ecker, and D. U. Sauer, "A holistic aging model for Li (NiMnCo) O2 based 18650 lithium-ion batteries," *Journal of Power Sources*, vol. 257, pp. 325–334, 2014.
[27] A. Kortsari, L. Mitropoulos, T. Heinemann, and H. Mikkelsen, "Prototype and full-scale demonstration of next-generation 100% electrically powered ferry for passengers and vehicles: Evaluation report of the e-ferry," 2020. [Online]. Available: https://cordis.europa.eu/project/id/636027/results
[28] R. Billinton, *Reliability evaluation of power systems*. Springer Science & Business Media, 1996.
[29] "IGBT modules," available:. [Online]. Available: https://www.infineon.com/cms/en/product/power/igbt/igbt-modules/.

Siamak Karimi (SM'20) was born in Shiraz, Iran, in 1994. He received his B.Sc. degree in electrical engineering from the University of Tehran, Tehran, Iran in 2016, and his M.Sc. in power electronics from the Sharif University of Technology, Tehran, Iran in 2019. He received his Ph.D. from the Norwegian University of Science and Technology (NTNU), Trondheim, Norway, in 2022. He is currently a senior R&D engineer at Eltek AS, Drammen, Norway. His research interests are the design, modeling, and control of power electronics systems used in electrified transportation, telecommunication, and data centers.

Mehdi Zadeh (M'11) received the Ph.D. degree in Electrical Engineering from the Norwegian University of Science and Technology (NTNU), Trondheim, Norway, in 2016. From 2016 to 2017, he was with Zaptec Charger, Stavanger, Norway, where he was working on the development of battery charging systems for electric vehicles based on wide band-gap power electronics. In 2017, he has joined the Department of Marine Technology at NTNU, Trondheim, where he is currently a Professor and the director of the Marine Electrification Research Lab. His current research interests include electrification for zero-emission and autonomous shipping, onboard and hybrid DC power systems, offshore renewable energy systems, and sustainable ports. He has taken part in the management of several European, national, and industrial projects, and is currently the work package leader for Power Systems and Fuel at the Norwegian Research-Based Innovation Centre for Improved Energy Efficiency and Reduced Harmful Emissions-called SFI Smart Maritime.

Jon Are Suul (M'11) received the M.Sc. degree in energy and environmental engineering and the Ph.D. degree in electric power engineering from the Norwegian University of Science and Technology (NTNU), Trondheim, Norway, in 2006 and 2012, respectively. From 2006 to 2007, he was with SINTEF Energy Research, Trondheim, where he was working with the simulation of power electronic converters and marine propulsion systems until starting his Ph.D. studies. Since 2012, he has been a Research Scientist with SINTEF Energy Research, first in a part-time position while working as a part-time Postdoctoral Researcher with the Department of Electric Power Engineering of NTNU until 2016. Since August 2017, he has been an Adjunct Associate Professor with the Department of Engineering Cybernetics, NTNU. His research interests are mainly related to modeling, analysis, and control of power electronic converters in power systems, renewable energy applications, and electrification of transport.